*Electronic Supporting Information*

# A versatile synthetic platform for amphiphilic nanogels with tunable hydrophobicity

**Alexandra Gruber,[a] Doğuş Işık,[a] Bianca Bueno Fontanezi,[b] Christoph Böttcher,[c] Monika Schäfer-Korting,[b] Daniel Klinger*[a]**

*[a] Institute of Pharmacy (Pharmaceutical Chemistry), Freie Universität Berlin,
Königin-Luise Str. 2-4, Berlin D-14195, Germany*
*[b] Institute of Pharmacy (Pharmacology and Toxicology), Freie Universität Berlin,
Königin-Luise Str. 2-4, Berlin D-14195, Germany*
*[c] Research Center of Electron Microscopy and CoreFacilty BioSupraMol, Institute of Chemistry and Biochemistry,
Freie Universität Berlin, Fabeckstr. 36a, Berlin D-14195, Germany*

*E-mail: daniel.klinger@fu-berlin.de*

**Content**

## 1. Investigation of swelling behavior of the precursor particles

The swelling behavior of the reactive PPFPMA precursor particles in DMF was investigated by DLS measurements. Here, the particle sizes in water and DMF were compared. The respective swelling ratio can be calculated as followed:

$$Q = \frac{V_{swollen}}{V_{non-swollen}}$$

The hydrodynamic diameter in water was determined by DLS measurements directly after copolymerization in miniemulsion. For measurements in DMF, purified, freeze-dried particles were dispersed in DMF and allowed to swell over night. As seen in Fig. S-1, DMF swells the polymer network of the particles and is therefore a suitable solvent for the fuctionalization reaction. The increase of the hydrodynamic diameter from 115 nm in water to 160 nm in DMF corresponds to a swelling ratio Q of 2.7. Meaning the volume of the particles nearly tripled.
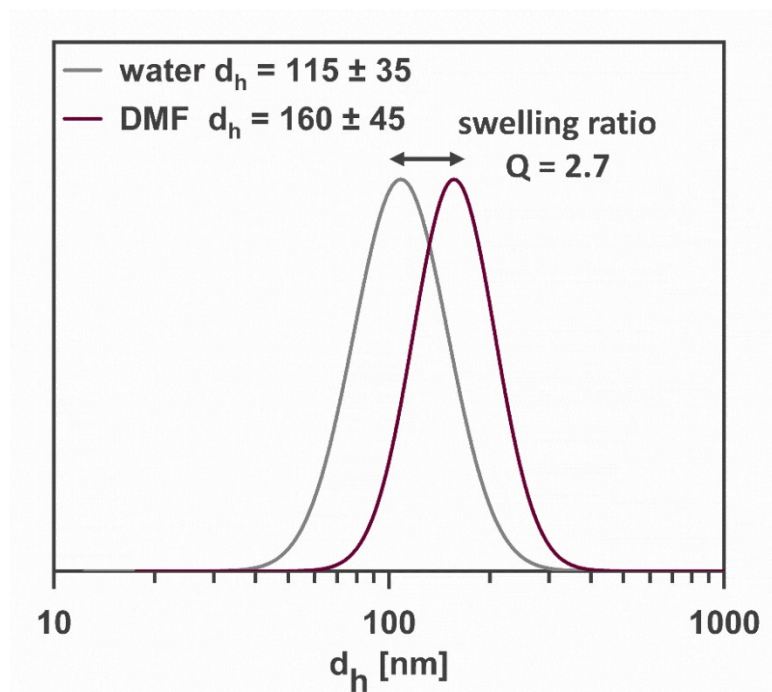


**Fig. S- 1** DLS plot of precursor particles in water and DMF, showing that DMF ensures a swollen PPFPMA network.

## 2. Monitoring the conversion of reactive PPFPMA network with hydrophilic and hydrophobic moieties

Conversion of the precursor particles into amphiphilic nanogels was monitored *via* attenuated total reflection fourier-transform infrared (ATR-FTIR) spectroscopy on freeze-dried nanogels. Fig. S-2 shows the successful conversion of the reactive PFP ester (1778 cm$^{-1}$) to the amide (1662 cm$^{-1}$) for amphiphilic nanogels of series 1 (20 mol-% hydrophobic moiety). In addition, quantitative conversion of the PFP ester groups was demonstrated for all nanogels by the disappearance of the PFP ester peaks in $^{19}$F-NMR spectra (Fig. S-3).
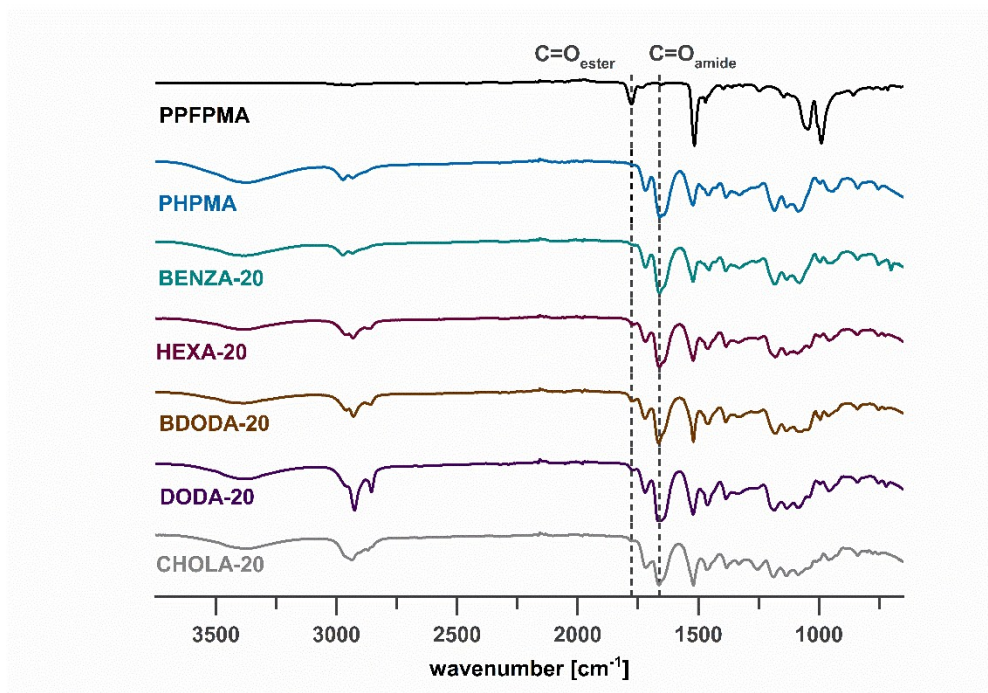


**Fig. S- 2** Successful network functionalization is demonstrated by the disappearance of the reactive PFP ester bands and the simultaneous appearance of the functionalized amide bands in ATR-FTIR spectra for nanogels of series 1.
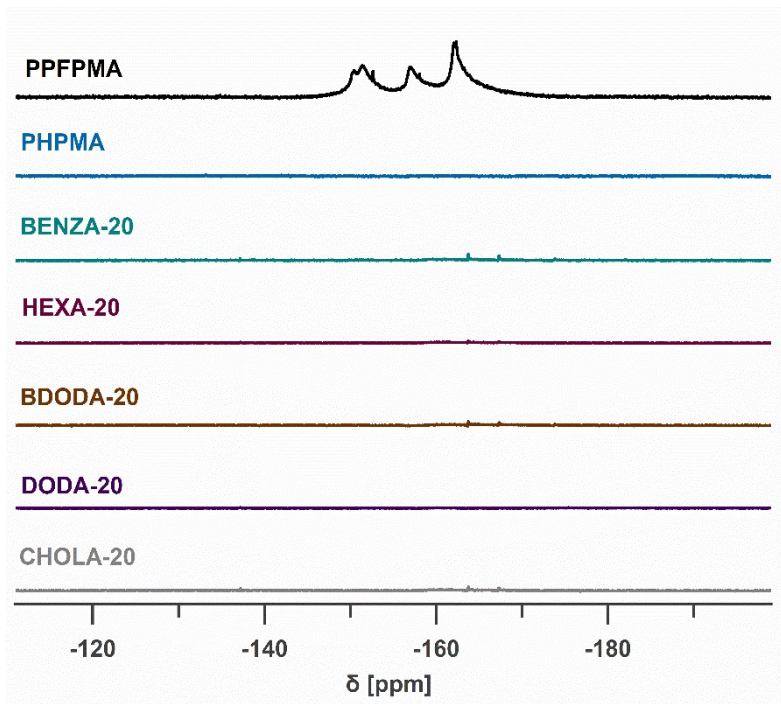


**Fig. S- 3** Successful network functionalization is demonstrated by the disappearance of PFP ester peaks in $^{19}$F-NMR spectra of nanogels of series 1.

### 3. Determination of incorporation efficiencies of functional moieties

Controlling the nanogel amphiphilicity requires the ability to tune the ratio between hydrophilic and hydrophobic moieties in the network. Synthetically, this was addressed by simply changing the ratio of the two different amines in the post-polymerization modification reaction. In order to determine incorporation efficiencies of the functional moieties into the particle network ^{1}H NMR spectroscopy was carried out. Incorporation values in the same range of the feed ratios were found, assuming similar reactivity of the different hydrophobic groups

**Table S- 1** Incorporation values of hydrophobic groups into nanogels determined by backbone integration closely resembled the targeted values (feed ratios).

| Hydrophobic group | Initial Feed [mol-%] | Found incorporated [mol-%] |
|---|---|---|
| BENZA | 20 | 23 |
| HEXA | 20 | 22 |
| BDODA | 20 | 24 |
| DODA | 20 | 23 |
| CHOLA | 20 | 20 |

(Table S-1).

Line broadening in the ^{1}H-NMR spectra limits the determination accuracy for the crosslinked nanogels (Fig. S-4).Thus, control experiments on linear polymer analogues[1] were performed to gain further insights into the efficiency of the functionalization reaction. For this, post-modification reactions of reactive precursor polymers were carried out with CHOLA as exemplary hydrophobe. As indicated in Fig. S-5 (complete spectra) the incorporated ratio of HPA/CHOLA moieties was determined via integration of respective peaks after deconvolution in the ^{1}H-NMR spectra.
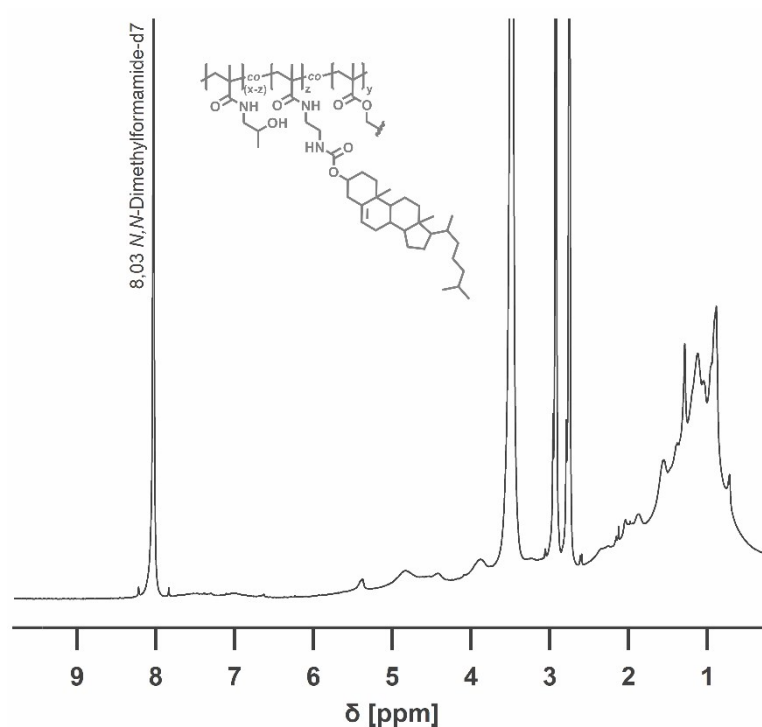


**Fig. S- 4** ^{1}H NMR spectra of CHOLA-20 nanogels in DMF-d7.
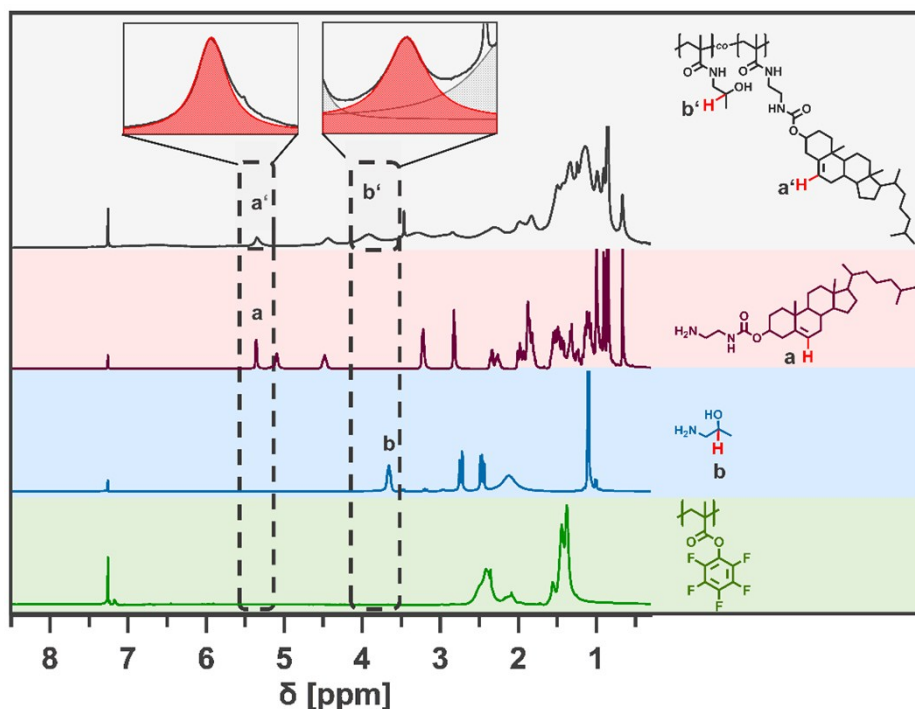
**Fig. S- 5** $^1$H NMR comparison of linear CHOLA-20 copolymer, and its functional moieties CHOLA and HPA as the PPFPMA polymer backbone reveals the presence of both functionalities in the copolymer, thus enabling quantitative analysis via integration after peak deconvolution (complete spectra).

It was demonstrated that changing the feed ratio of both amines (HPA and CHOLA) allows tuning the network composition: the experimental incorporation values for CHOLA show a linear relationship to the initially added feed (simultaneous addition). To account for potential differences in reactivity between CHOLA and HPA, control experiments with the sequential addition of the amines were performed. For this, the polymer was first reacted with 0.1-0.5 equivalents of CHOLA. Second, after 24 hours, remaining active PFP esters on the polymer were quenched with an excess of HPA. The incorporation results were similar to the simultaneous addition (Fig. S-6). In addition, we observed aggregation of the polymers upon the first functionalization with CHOLA in solution. Thus, it becomes obvious that the simultaneous functionalization strategy is the method of choice for the
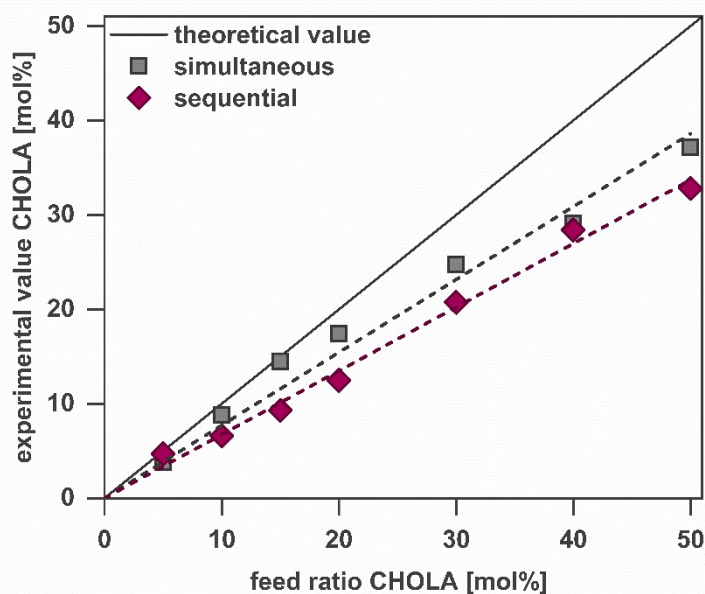


**Fig. S- 6** Incorporation efficiencies of CHOLA by simultaneous and sequential post-modification of linear PPFPMA polymers show good correlation between feed ratio and incorporation.

5

generation of amphiphilic nanogels. In this approach, the hydrophilic/hydrophobic ratio can accurately be controlled by simply varying the feed ratio of the two added amines.

## 4. Transmission electron microscopy (TEM)

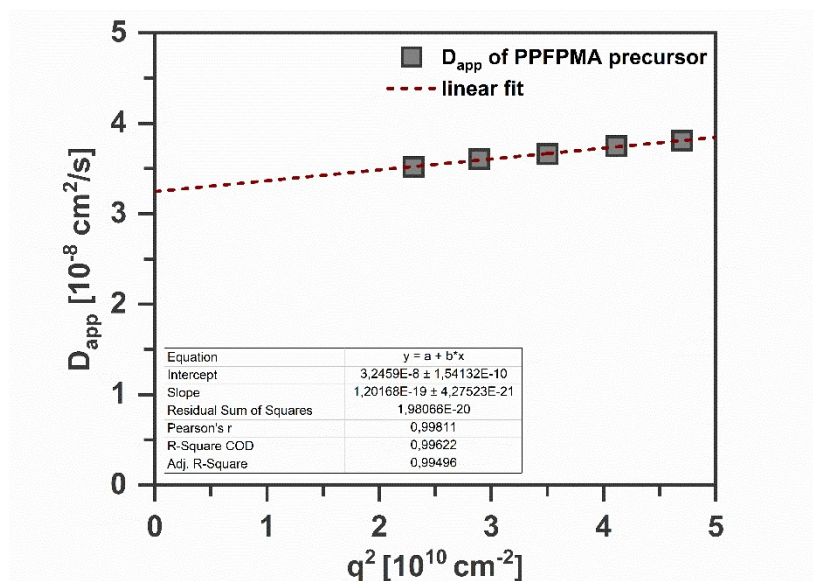TEM measurments of nanogels different hydrophobicity, show well defined nanogels with narrow size
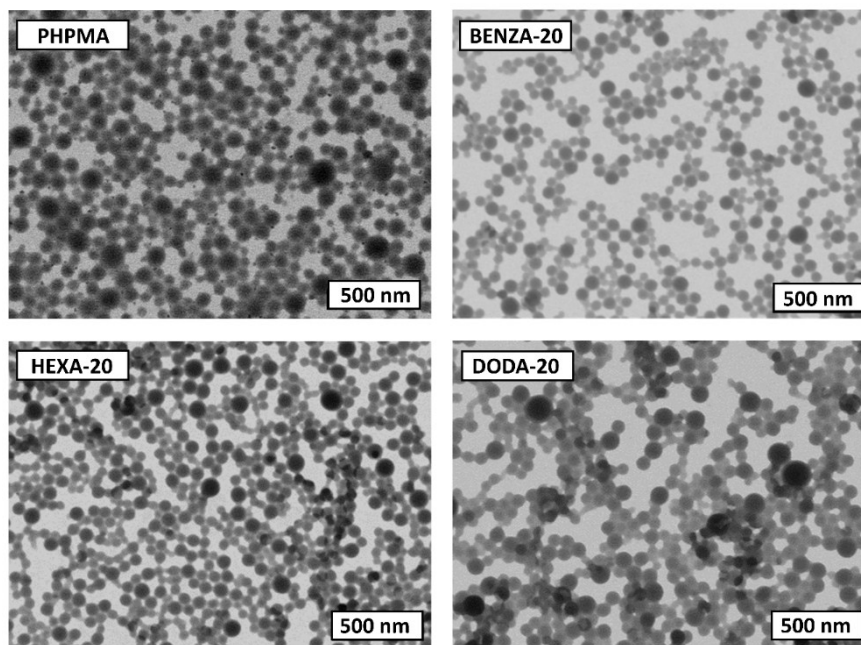


**Fig. S- 7** TEM images of amphiphilic nanogels of different hydrophobic group, showing defined nanogels.

distributions Fig. S-7 .

## 5. Particle characterization by angle-dependent dynamic light scattering

Particle size distributions were determined by dynamic light scattering, performed on a Nicomp Nano Z3000 (Particle Sizing Systems, Port Richey, United Stated of America). The measurements were carried out at room temperature on diluted dispersions in the respective solvents.

Angle-dependent measurements were carried out at scattering angles of 70°, 80°, 90°, 100° and 110°. The apparent diffusion coefficient $D_{app}$ was provided by the Nicomp Nano Z3000 by cumulant analysis of the autocorrelation function and plotted against the quadratic scattering vector $q^2$. By extrapolation of the plotted data to the y-intercept, the z-average diffusion coefficient $D_s$ was obtained (Fig. S-8). $D_s$ was used to calculate the hydrodynamic diameter of the nanogels.



| Equation | y = a + b*x |
|---|---|
| Intercept | 3,2459E-8 ± 1,54132E-10 |
| Slope | 1,20168E-19 ± 4,27523E-21 |
| Residual Sum of Squares | 1,98066E-20 |
| Pearson's r | 0,99811 |
| R-Square COD | 0,99622 |
| Adj. R-Square | 0,99496 |

**Fig. S- 8** Z-average diffusion coefficient $D_s$ obtained by extrapolation to the y-intercept of the apparent diffusion coefficient $D_{app}$ plotted against the quadratic scattering vector $q^2$. Representative shown for PPFPMA precursor particles.

## 6. Investigation of Swelling Behavior

In order to get a rough estimate on the swelling properties of the amphiphilic nanogels the degree of swelling is determined by calculating the volume ratio of the swollen nanogels compared to the non-swollen, dried nanogels:

$$Q = \frac{V_{swollen}}{V_{non-swollen}}$$

The volume of the non-swollen nanogels was determined by evaluating TEM images of the respective dried nanogels. The diameter of 200 nanogels of each sample was determined with the software ImageJ (version 1.52e). The evaluation of TEM images showed similar sizes and size distributions for nanogels with different network amphiphilicity. These are very similar in size to the reactive precursor particles (Fig. S-9).
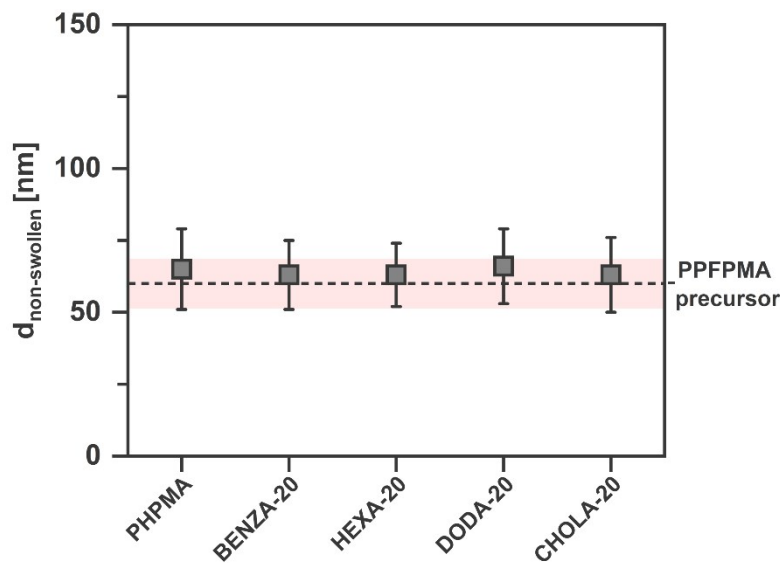


**Fig. S- 9** TEM evaluation of nanogels with different network amphiphilicity show similar size and size distribution in a non-swollen state. The dotted line represents the diameter of the reactive precursor particles and the coloured box the respective standard deviation.

The volume of the swollen nanogels was calculated from the hydrodynamic radius determined by angle-dependent DLS measurements. Using the hydrodynamic radius in comparison to the dried state will lead to an overestimation of the swelling ratios of the nanogels but gives a rough approximation. Degrees of swelling are shown in Fig. S-10a.
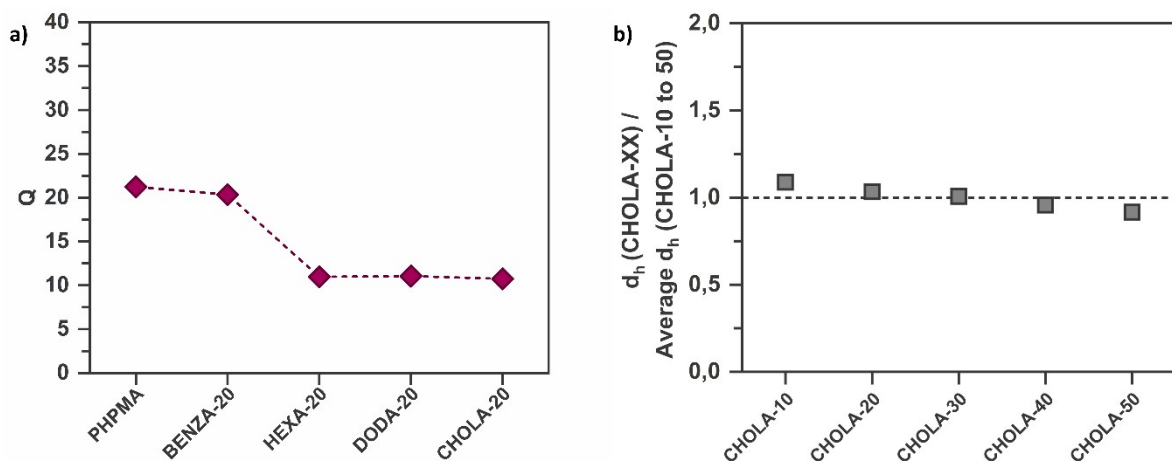


**Fig. S- 10** The swelling ration of the amphiphilic nanogels decrease with increasing hydrophobicity. The decreased swelling ability is assumed to be due to additional physical crosslinks formed by the hydrophobic groups. (a) Degree of swelling of amphiphilic nanogels different hydrophobic pendant groups. (b) Relative deviation of the size of each CHOLA nanogel from the average size of all CHOLA nanogels (series 2).
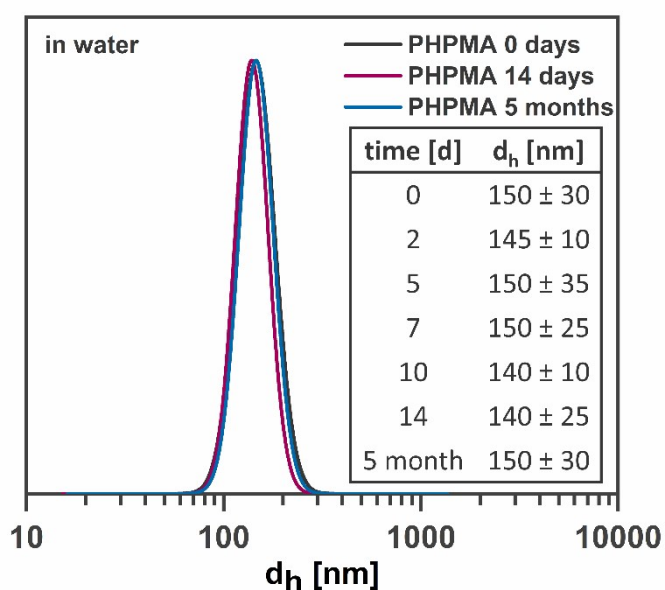
By increasing the hydrophobic content in the networks, a gradual transition from nanogels to rigid nanoparticles is likely to occur. A distinct differentiation between solid nanoparticles and slightly swollen nanogels represents a challenge. One way to address this task is to investigate the nanogel size in aqueous medium: More hydrophobic nanogels should swell less due to a reduced hydration of the network polymer. Thus, the nanogel size and degree of swelling should decrease slightly with increasing network hydrophobicity. However, this effect additionally depends on the overall ability to swell as determined by the crosslinker amount. The presented nanogels contain a relatively high amount of 5 mol% crosslinker which already limits the swelling to a certain degree.

The slight reduction in the nanogel size and degree of swelling can be observed for the set of amphiphilic nanogels functionalized with 80 mol% hydrophilic HPA and 20 mol% of varying hydrophobic groups. Here, purely hydrophilic PHPMA nanogels are larger than the hydrophobically modified nanogels. However, it can be seen that for log P values higher than BENZA, almost no further deviation of nanogel size and degree of swelling can be observed (Fig. 4a, Fig. S-10a). It is suggested that in these cases the additional increase in network hydrophobicity is not enough to cause any further significant deviations in swelling.

This translates to the set of nanogels with an increasing CHOLA content (series 2, Table 1). While amphiphilic nanogels with 20 mol% CHOLA are smaller than the hydrophilic PHPMA nanogels, further increasing the CHOLA content does not translate to any further significant changes in nanogel size: measuring the size of nanogels with different amounts of hydrophobic CHOLA (feed up to 50 mol%) showed only a minor reduction of nanogel size with increasing CHOLA content and comparable size distributions. To illustrate the similarity of the different CHOLA-functionalized nanogels, the relative size deviation of each nanogel from the average size of the nanogel series 2 was plotted in Fig. S-10b. However, as discussed in the following section, all nanogels with CHOLA feeds up to 50 mol% showed high colloidal stability upon prolonged storage in aqueous medium (more than two weeks). This suggests a dominating hydrophilic character of the nanogels. In contrast, nanogels with CHOLA incorporation ratios of more than 50 mol% were not stable in water (data not shown).

## 7. Stability measurements

The colloidal stability of the nanogels was determined for dispersions of nanogels in ultrapure water (c = 1 mg/mL). Monitoring the nanogel size by DLS at an angle of 173° over a time period of 14 days showed no significant changes in the overall hydrodynamic diameters. Only slight reversible deviations in the size distribution, e.g. broadening or narrowing over time, were observed, thus suggesting good colloidal stability. Fig. S-11 to Fig. S-20 show that all nanogels are stable for more than 14 days in water. For selected nanogels (PHPMA, HEXA-20 and CHOLA-20) colloidal stability for a minimum of five months was demonstrated (Fig. S-11, Fig. S-13 and Fig. S-16 To evaluate the colloidal stability of the nanogels under physiological model conditions lyophilized nanogels of series 1 Table 1. were dispersed in phosphate-buffered saline (PBS) and Dulbecco's Modified Eagle Medium (c = 1mg/mL). All nanogels are stable for the measured time period of 14 days (Fig. S-21 to Fig. S-32).
By increasing the hydrophobic content in the nanogels a gradual transition from nanogels to rigid nanoparticles is likely to occur. A distinct differentiation between solid nanoparticles and slightly swollen nanogels represents a challenge. Besides investigating the particle size and swelling ratio of the nanogels (discussed in the previous section), colloidal stability is an indication for a hydrophilic character. Nanogels with CHOLA incorporation up to 50 mol% showed high colloidal stability upon prolonged storage in aqueous medium (more than two weeks). This suggests a dominating hydrophilic character of the nanogels. In contrast, nanogels with incorporation ratios of more than 50 mol% were not stable in water, thus suggesting a predominantly hydrophobic nature (data not shown).



| in water | PHPMA 0 days / PHPMA 14 days / PHPMA 5 months |
|---|---|

| time [d] | $d_h$ [nm] |
|---|---|
| 0 | 150 ± 30 |
| 2 | 145 ± 10 |
| 5 | 150 ± 35 |
| 7 | 150 ± 25 |
| 10 | 140 ± 10 |
| 14 | 140 ± 25 |
| 5 month | 150 ± 30 |

**Fig. S- 11** DLS curves of PHPMA nanogels after 0 days, 14 days and five months show colloidal stable nanogels in water. Measurements are carried out at an angle of 173°. Error values represents the width of the size distribution as full width at half maximum (FWHM).
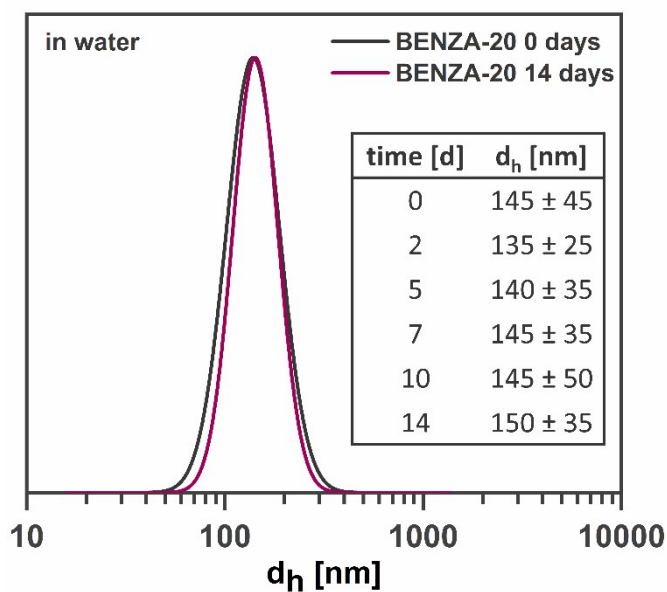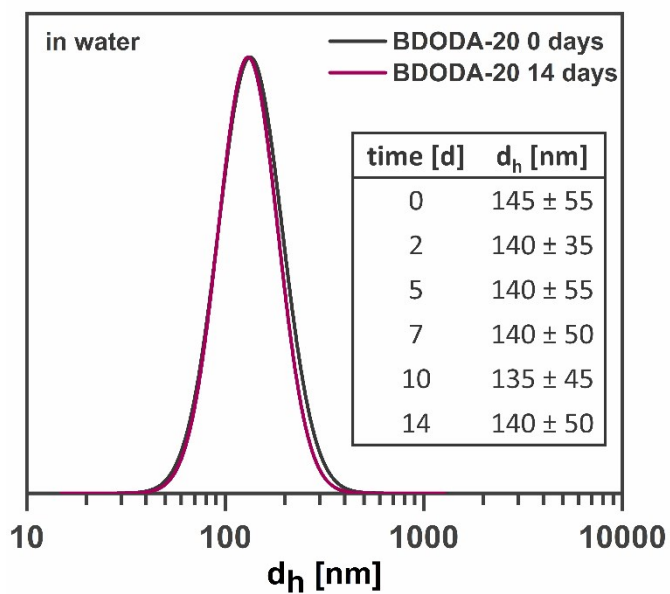
**Fig. S- 12** DLS curves of BENZA-20 nanogels after 0 and 14 days show colloidal stable nanogels in water. Measurements are carried out at an angle of 173°. Error values represents the width of the size distribution as full width at half maximum (FWHM).
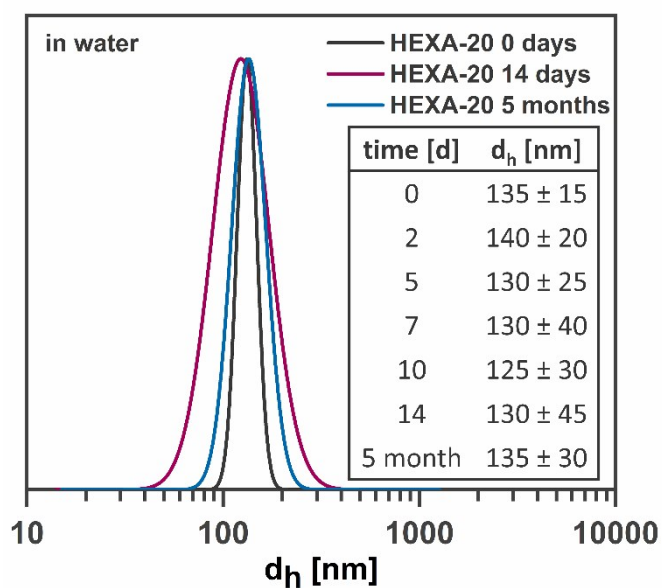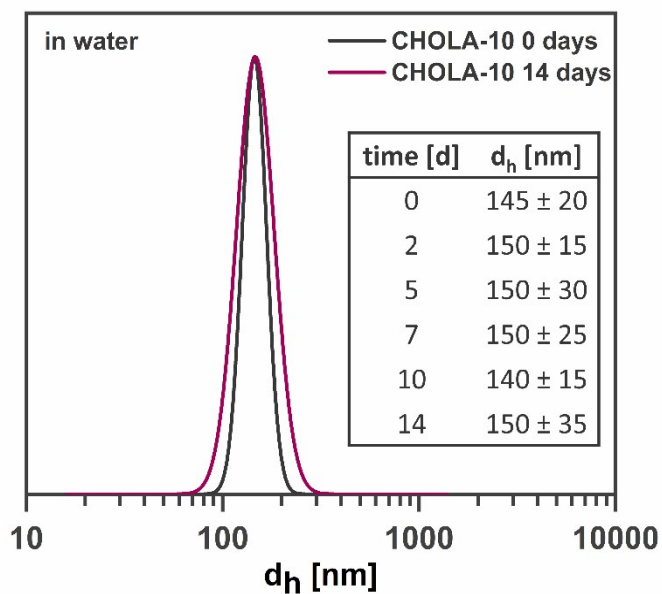


**Fig. S- 13** DLS curves of HEXA-20 nanogels after 0 days, 14 days and five months show colloidal stable nanogels in water. Measurements are carried out at an angle of 173°. Error values represents the width of the size distribution as full width at half maximum (FWHM).

11
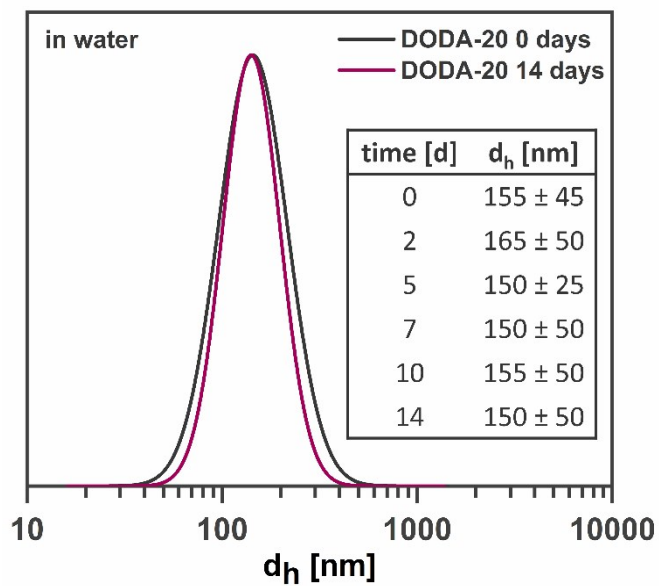
**Fig. S- 14** DLS curves of DODA-20 nanogels after 0 and 14 days show colloidal stable nanogels in water. Measurements are carried out at an angle of 173°. Error values represents the width of the size distribution as full width at half maximum (FWHM).
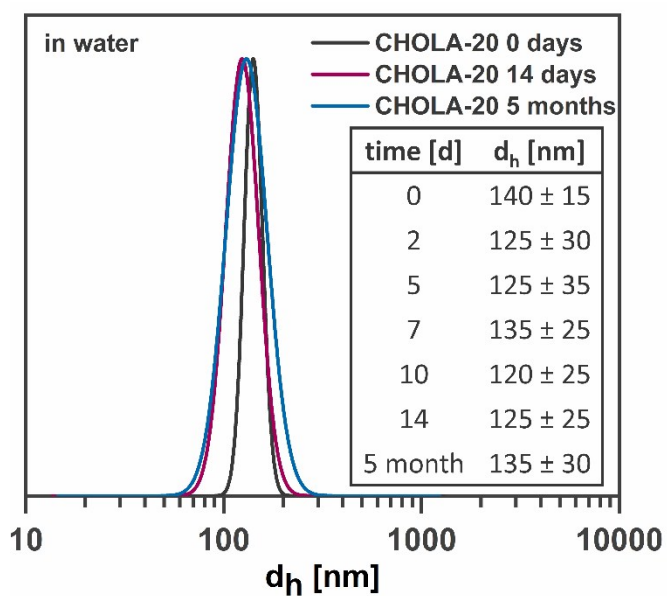


**Fig. S- 15** DLS curves of BDODA-20 nanogels after 0 and 14 days show colloidal stable nanogels in water. Measurements are carried out at an angle of 173°. Error values represents the width of the size distribution as full width at half maximum (FWHM).

| time [d] | $d_h$ [nm] |
|----------|------------|
| 0 | 145 ± 20 |
| 2 | 150 ± 15 |
| 5 | 150 ± 30 |
| 7 | 150 ± 25 |
| 10 | 140 ± 15 |
| 14 | 150 ± 35 |

**Fig. S- 16** DLS curves of CHOLA-10 nanogels after 0 and 14 days show colloidal stable nanogels in water. Measurements are carried out at an angle of 173°. Error values represents the width of the size distribution as full width at half maximum (FWHM).



| time [d] | $d_h$ [nm] |
|----------|------------|
| 0 | 140 ± 15 |
| 2 | 125 ± 30 |
| 5 | 125 ± 35 |
| 7 | 135 ± 25 |
| 10 | 120 ± 25 |
| 14 | 125 ± 25 |
| 5 month | 135 ± 30 |

**Fig. S- 17** DLS curves of CHOLA-20 nanogels after 0 days, 14 days and five months show colloidal stable nanogels in water. Measurements are carried out at an angle of 173°. Error values represents the width of the size distribution as full width at half maximum (FWHM).
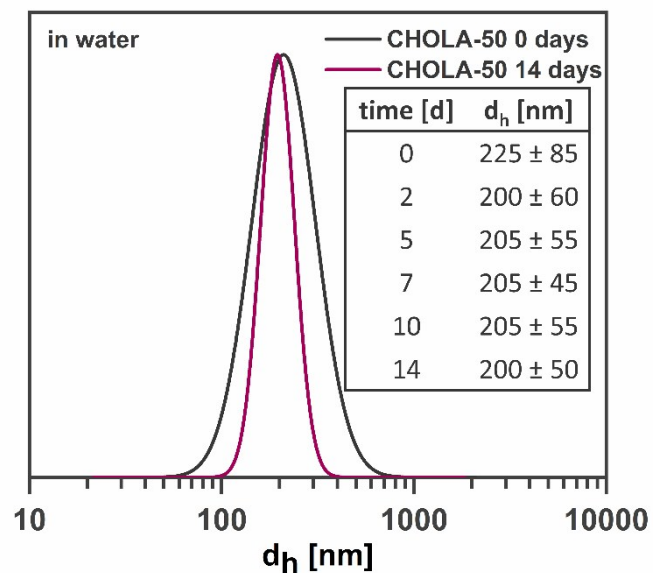
13
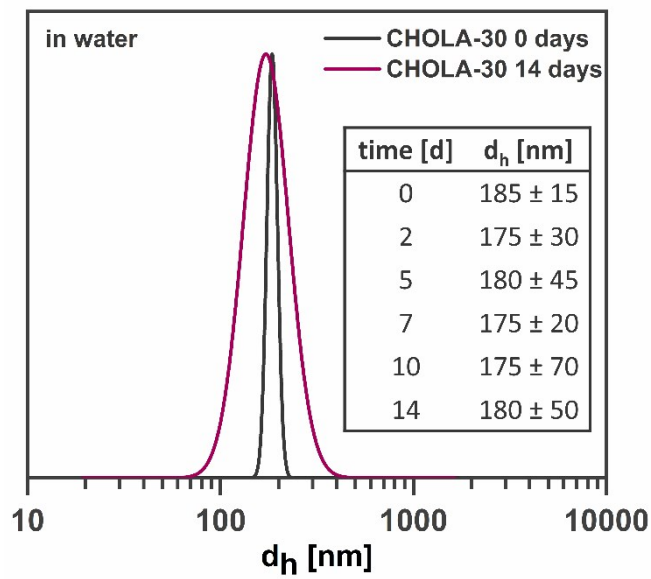
**Fig. S- 18** DLS curves of CHOLA-30 nanogels after 0 and 14 days show colloidal stable nanogels in water. Measurements are carried out at an angle of 173°. Error values represents the width of the size distribution as full width at half maximum (FWHM).
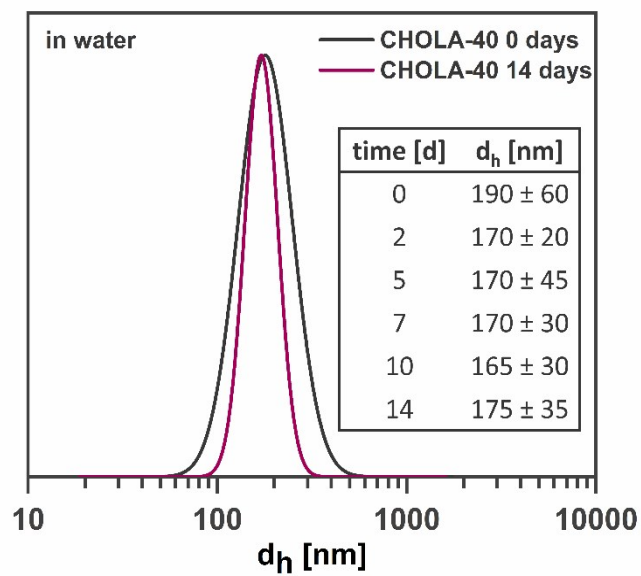


**Fig. S- 19** DLS curves of CHOLA-40 nanogels after 0 and 14 days show colloidal stable nanogels in water. Measurements are carried out at an angle of 173°. Error values represents the width of the size distribution as full width at half maximum (FWHM).
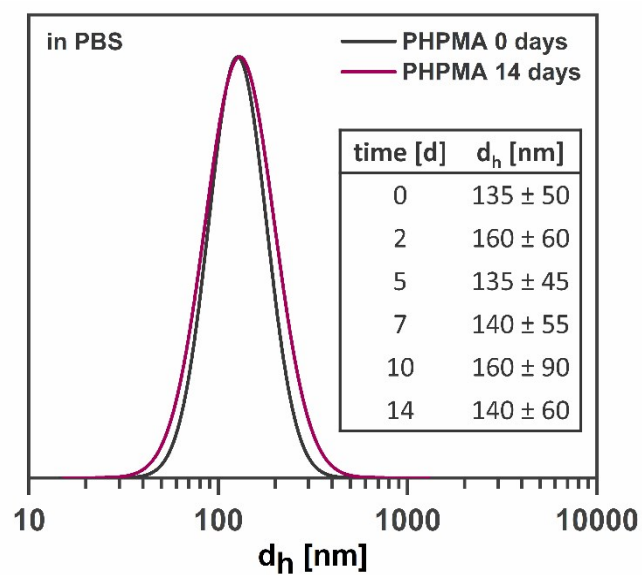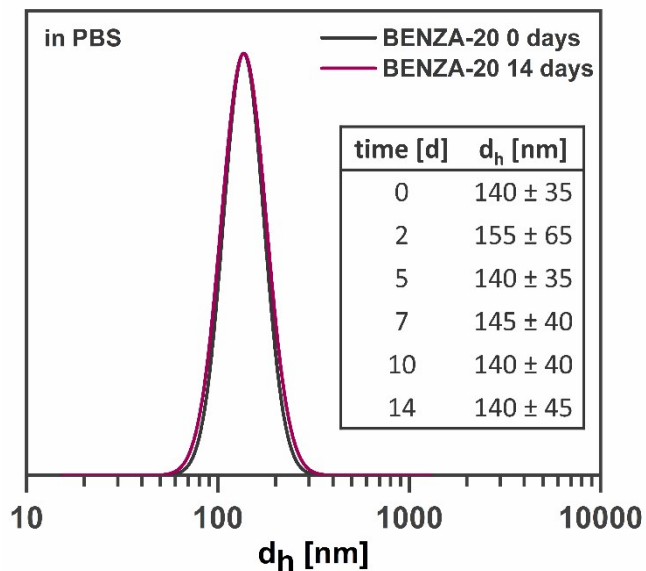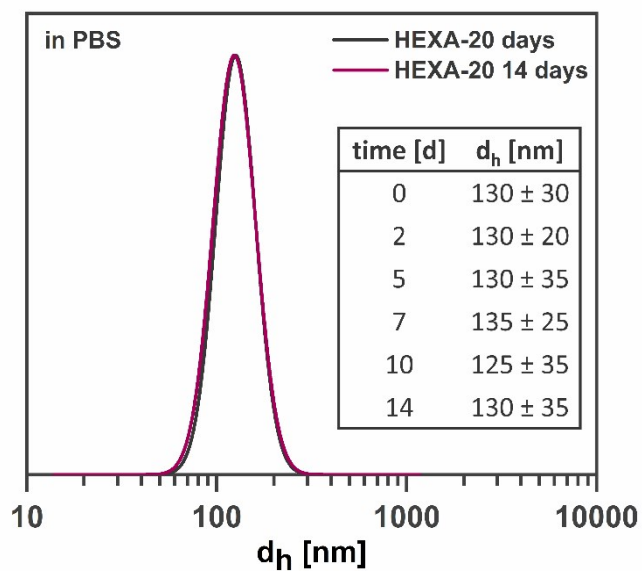
**Fig. S- 20** DLS curves of CHOLA-50 nanogels after 0 and 14 days show colloidal stable nanogels in water. Measurements are carried out at an angle of 173°. Error values represents the width of the size distribution as full width at half maximum (FWHM).



**Fig. S- 21** DLS curves of PHPMA nanogels after 0 and 14 days show colloidal stable nanogels in PBS. Measurements are carried out at an angle of 173°. Error values represents the width of the size distribution as full width at half maximum (FWHM).

**Fig. S- 22** DLS curves of BENZA-20 nanogels after 0 and 14 days show colloidal stable nanogels in PBS. Measurements are carried out at an angle of 173°. Error values represents the width of the size distribution as full width at half maximum (FWHM).



**Fig. S- 23** DLS curves of HEXA-20 nanogels after 0 and 14 days show colloidal stable nanogels in PBS. Measurements are carried out at an angle of 173°. Error values represents the width of the size distribution as full width at half maximum (FWHM).
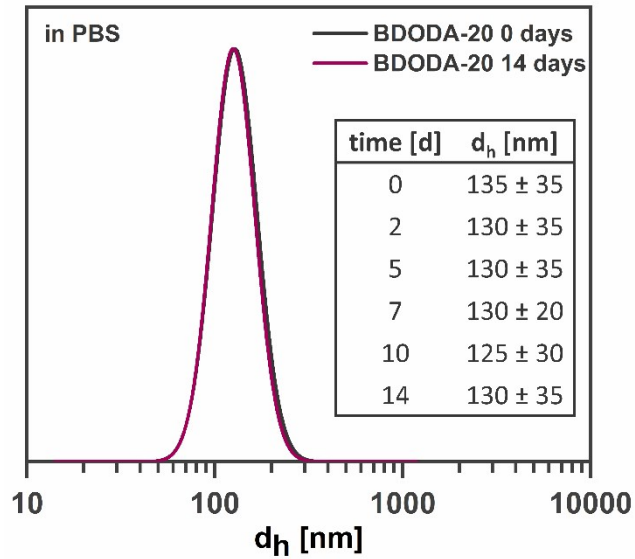
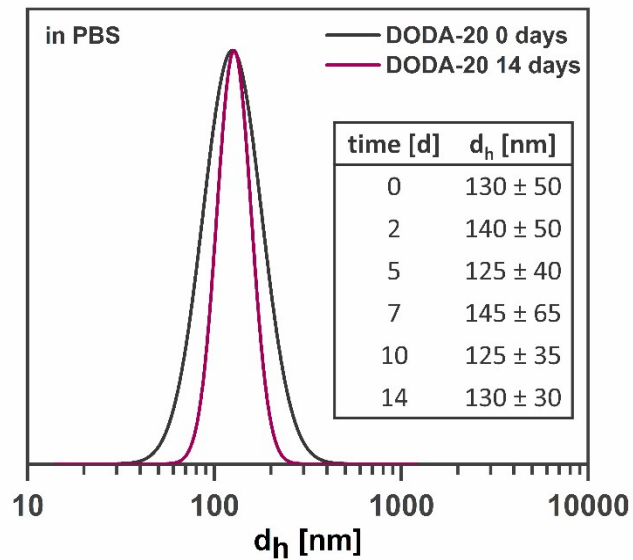| time [d] | $d_h$ [nm] |
|----------|-----------|
| 0 | 135 ± 35 |
| 2 | 130 ± 35 |
| 5 | 130 ± 35 |
| 7 | 130 ± 20 |
| 10 | 125 ± 30 |
| 14 | 130 ± 35 |

**Fig. S- 24** DLS curves of BDODA-20 nanogels after 0 and 14 days show colloidal stable nanogels in PBS. Measurements are carried out at an angle of 173°. Error values represents the width of the size distribution as full width at half maximum (FWHM).



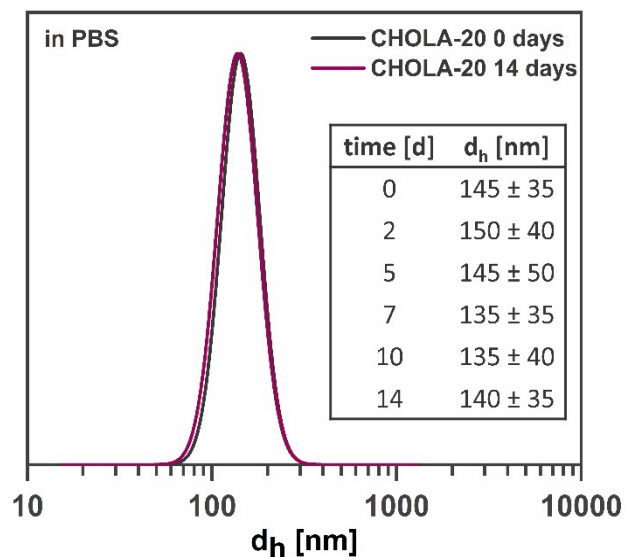| time [d] | $d_h$ [nm] |
|----------|-----------|
| 0 | 130 ± 50 |
| 2 | 140 ± 50 |
| 5 | 125 ± 40 |
| 7 | 145 ± 65 |
| 10 | 125 ± 35 |
| 14 | 130 ± 30 |

**Fig. S- 25** DLS curves of DODA-20 nanogels after 0 and 14 days show colloidal stable nanogels in PBS. Measurements are carried out at an angle of 173°. Error values represents the width of the size distribution as full width at half maximum (FWHM).
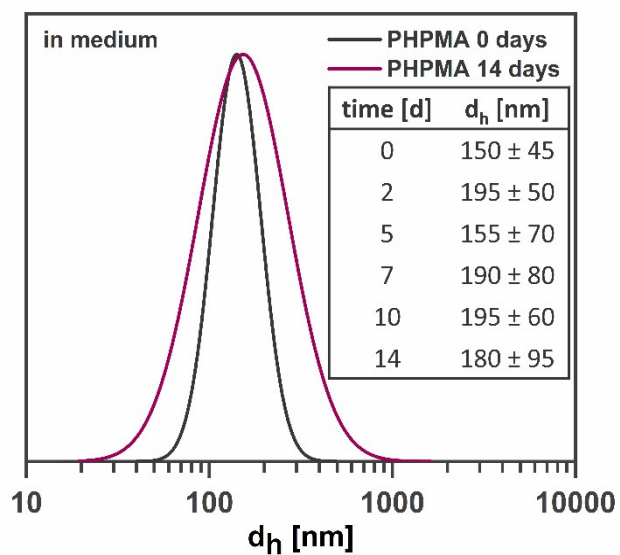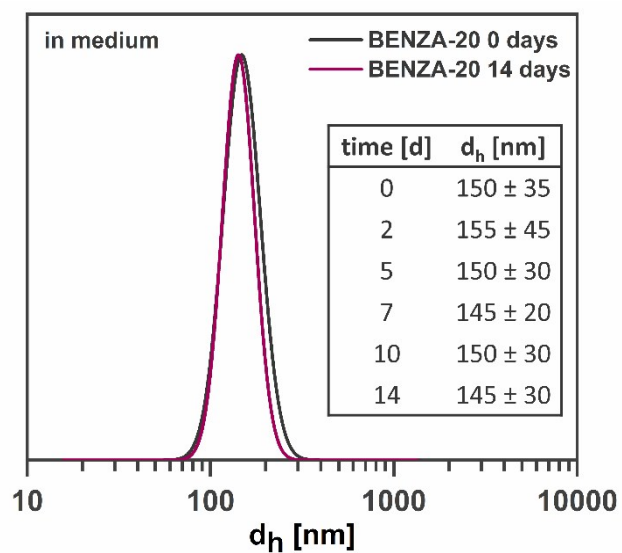
**Fig. S- 26** DLS curves of CHOLA-20 nanogels after 0 and 14 days show colloidal stable nanogels in PBS. Measurements are carried out at an angle of 173°. Error values represents the width of the size distribution as full width at half maximum (FWHM).



**Fig. S- 27** DLS curves of PHPMA nanogels after 0 and 14 days show colloidal stable nanogels in medium. Measurements are carried out at an angle of 173°. Error values represents the width of the size distribution as full width at half maximum (FWHM).

| time [d] | $d_h$ [nm] |
|---|---|
| 0 | 150 ± 35 |
| 2 | 155 ± 45 |
| 5 | 150 ± 30 |
| 7 | 145 ± 20 |
| 10 | 150 ± 30 |
| 14 | 145 ± 30 |

**Fig. S- 28** DLS curves of BENZA-20 nanogels after 0 and 14 days show colloidal stable nanogels in medium. Measurements are carried out at an angle of 173°. Error values represents the width of the size distribution as full width at half maximum (FWHM).



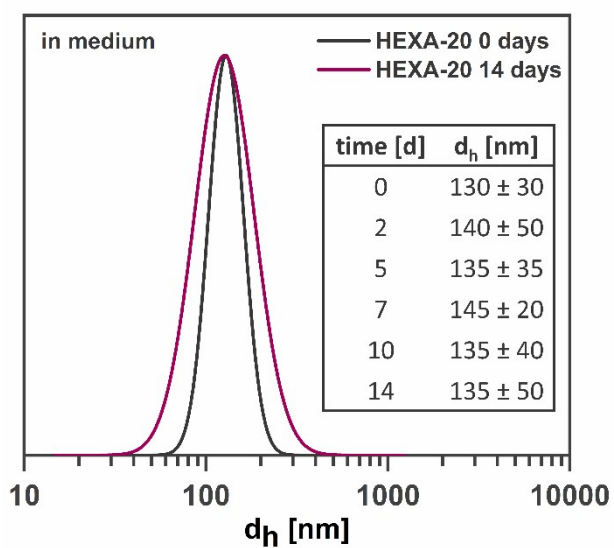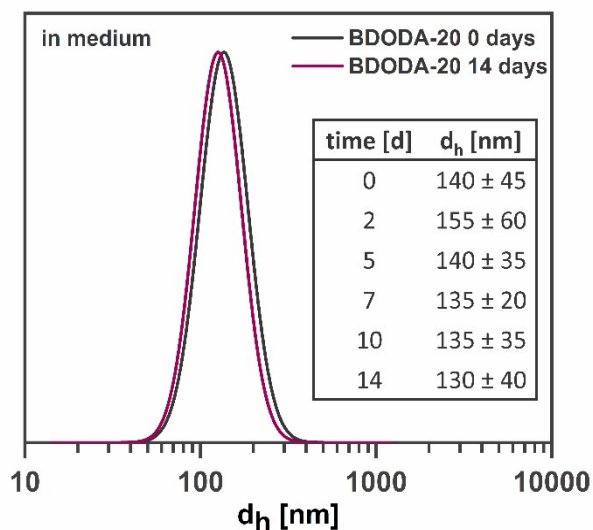| time [d] | $d_h$ [nm] |
|---|---|
| 0 | 130 ± 30 |
| 2 | 140 ± 50 |
| 5 | 135 ± 35 |
| 7 | 145 ± 20 |
| 10 | 135 ± 40 |
| 14 | 135 ± 50 |

**Fig. S- 29** DLS curves of HEXA-20 nanogels after 0 and 14 days show colloidal stable nanogels in medium. Measurements are carried out at an angle of 173°. Error values represents the width of the size distribution as full width at half maximum (FWHM).

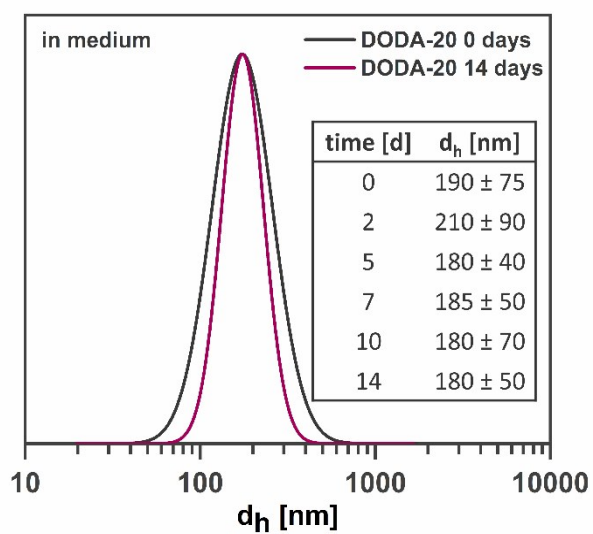| time [d] | $d_h$ [nm] |
|---|---|
| 0 | 140 ± 45 |
| 2 | 155 ± 60 |
| 5 | 140 ± 35 |
| 7 | 135 ± 20 |
| 10 | 135 ± 35 |
| 14 | 130 ± 40 |

**Fig. S- 30** DLS curves of BDODA-20 nanogels after 0 and 14 days show colloidal stable nanogels in medium. Measurements are carried out at an angle of 173°. Error values represents the width of the size distribution as full width at half maximum (FWHM).



| time [d] | $d_h$ [nm] |
|---|---|
| 0 | 190 ± 75 |
| 2 | 210 ± 90 |
| 5 | 180 ± 40 |
| 7 | 185 ± 50 |
| 10 | 180 ± 70 |
| 14 | 180 ± 50 |

**Fig. S- 31** DLS curves of DODA-20 nanogels after 0 and 14 days show colloidal stable nanogels in medium. Measurements are carried out at an angle of 173°. Error values represents the width of the size distribution as full width at half maximum (FWHM).
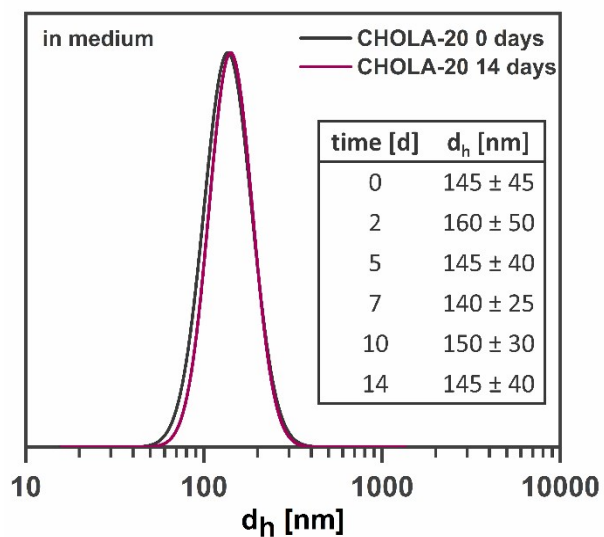
**Fig. S- 32** DLS curves of CHOLA-20 nanogels after 0 and 14 days show colloidal stable nanogels in medium. Measurements are carried out at an angle of 173°. Error values represents the width of the size distribution as full width at half maximum (FWHM).

## 8. Investigation of the nanogels loading behavior

To investigate the influence of the amphiphilicity of the nanogels on their loading behavior, the dye Nile red was used as a hydrophobic model compound. Encapsulation of Nile red was performed using the co-solvent method. Aqueous dispersions of the respective nanogels were mixed with a solution of Nile red in acetone. The organic solvent was then evaporated, causing the incorporation of the hydrophobic dye into the nanogels. After the loading process, the particle dispersions were filtered over cotton to remove excess of precipitated Nile red. This was followed by a second filtering step over 0.8 µm cellulose mixed ester syringe filters. TEM images of loaded, filtered nanogels did not show any Nile red aggregates (Fig. S- 33). Nile red was quantified by UV/VIS measurements on freeze-dried nanogels, redispersed in dimethylsulfoxide (DMSO) relative to a Nile red calibration curve (Fig. S- 34). As Nile red has some solubility in water, a blank sample analog to the normal samples was prepared to determine the natural solubility of Nile red in water (Optical spectra; Fig. S- 35). The solubility obtained from this blank control was subtracted from the nanocarrier results to obtain the effective loading.

The LCs of the nanogels of series 1 consisting of around 80 mol-% hydrophilic PHPMA with 20 mol-% incorporation of different hydrophobic groups were compared by plotting the LC against the calculated logP values of the incorporated hydrophobic structural unit (calculated from www.molinspiration.com). Table S- 2 shows the structural units used for the calculation and the corresponding calculated logP values.



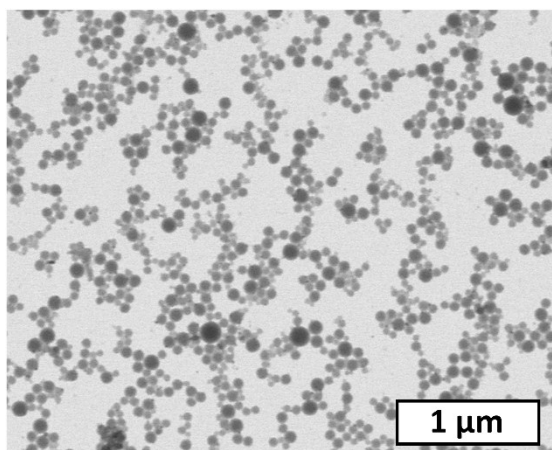**Fig. S- 33** Nile red loaded CHOLA-20 nanogels (filtered CME 0.8 µm) did not show any Nile red aggregates.
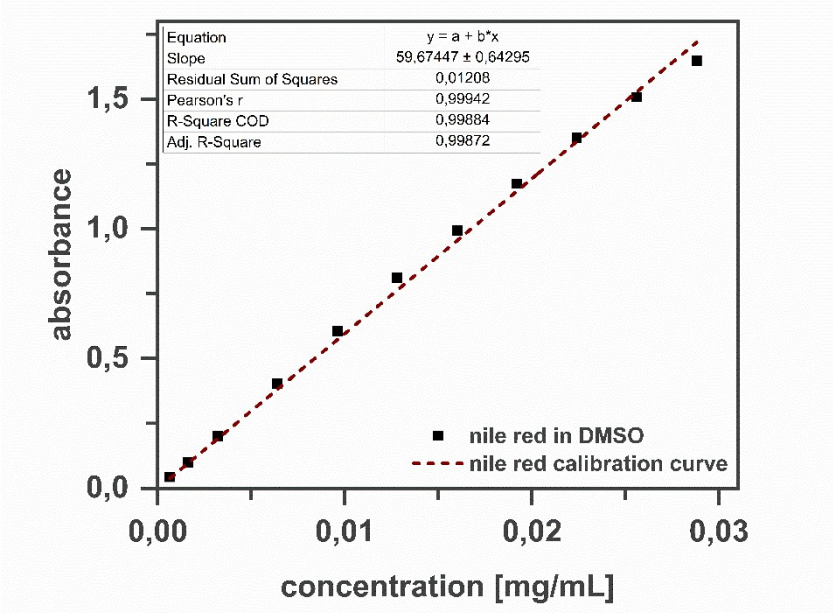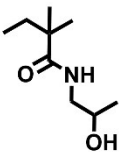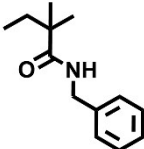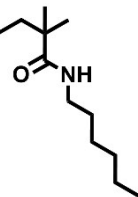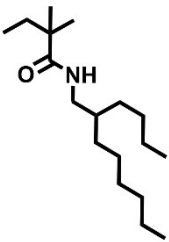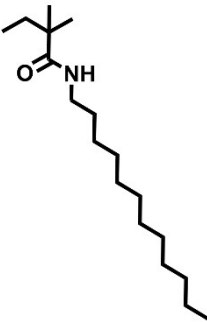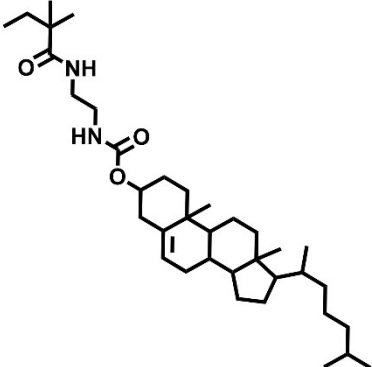


**Fig. S- 34** Calibration curve of Nile red in DMSO at 552 nm.
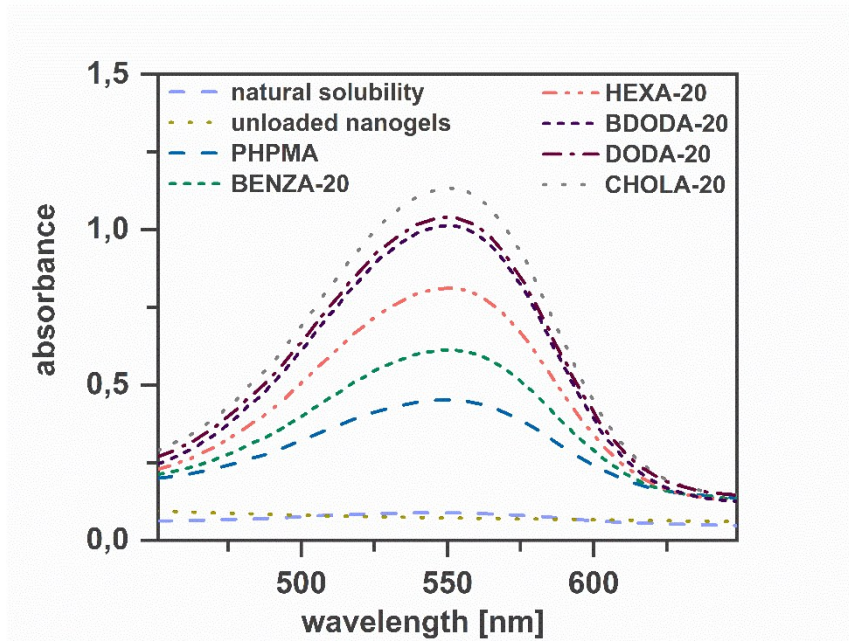
**Fig. S- 35** Optical spectra of nanogels loaded with Nile red compared to unloaded ones and the natural solubility of Nile red in water.

**Table S- 2** Structural unit for calculation of logP (calculated from www.molinspiration.com).

| functional group | structural unit for logP calculation | calculated logP |
|---|---|---|
| HPA |  | 1.52 |
| BENZA |  | 3.18 |
| HEXA |  | 4.23 |
| BDODA |  | 7.05 |
| DODA |  | 7.26 |
| CHOLA |  | 8.86 |

### 9. Materials and Methods

**Materials**

Methacryloyl chloride (97%) and Pentafluorophenol (99%) was purchased from ABCR. 1-Dodecylamine (97%), n-hexadecane (99%) and cholesteryl chloroformate was purchased from Alfa Aesar. Sodium dodecyl sulfate and ethylene glycol dimethacrylate (> 97,5%) were purchase from Merck. (2,2'-Azobis(2-methylpropionitrile) (98%), benzylamine (99%), hexylamin (99%) and Dulbecco's Modified Eagle Medium was purchased from Sigma-Adrich. 2-butyl-n-octan-1-amin (BDODA) (>98%) was purchased from TCI and Nile red from fluorochem. Anhydrous solvents were taken from MBraun MB SPS-800 solvent purification system and ultrapure water from LaboStar UV 2 water system. PFPMA,[1, 2] PPFPMA,[1] CHOLA[3, 4] and post-modification of PPFPMA[5] were performed according to literature procedures. Moisture or air sensitive reactions were carried out in dry glassware under nitrogen atmosphere. Dialysis was performed in benzoylated cellulose dialysis tubes from Sigma-Aldrich (width: 32 mm, MWCO 2000g mol$^{-1}$).

**Synthesis:**

**Synthesis of pentafluorophenyl methacrylate (PFPMA)[1, 2]** Pentafluorophenol (16.57 g, 90.0 mmol, 1.0 eq) and 2,6-lutidin (10.5 mL, 92.0 mmol, 1.0 eq) were dissolved in 150 mL DCM and cooled to 0 °C. Under cooling, 8.8 mL methacryloyl chloride (90.1 mmol, 1.0 eq) was slowly added. The reaction mixture was stirred for 3 hours at 0 °C before removing the ice bath and stirring the reaction mixture over night. The solution was filtered to remove precipitated 2,6-lutidine hydrochloride. The filtrate was washed three times with 100 mL water and once with $NH_4Cl$ before drying over $MgSO_4$. A small amount (ca. 100 mg) of di-tert-butyl-*p*-cresol was added to prevent polymerization during the next steps. The solvent was removed and the remaining liquid distilled under reduced pressure (0.02 mbar, 26 - 27 °C boiling point). Pentafluorophenyl methacylate was obtained as a colorless liquid (14.11 g, 55.9 mmol, 62 % yield).$^1$H NMR (400 MHz, $CDCl_3$): δ = 6.45 (s, 1H, **H**$_{cis}$), 5.91 (s, 1H, **H**$_{trans}$), 2.09 (s, 3H, C**H**$_3$) ppm; $^{19}$F NMR (376 MHz, $CDCl_3$): δ = -152.71 (d, *J* = 18.5 Hz, 2F, F$_{ortho}$), -158.14 (t, *J* = 21.3 Hz, 1 F, F$_{para}$), -162.43 (t, *J* =20.4 Hz, 2F, F$_{meta}$) ppm.

**Synthesis of amine functionalized cholesteryl (CHOLA)[3, 4]** In a predried schlenk flask 5.04 g cholesteryl chloroformate (11.2 mmol, 1.0 eq) was dissolved in 20 mL anhydrous DCM and added dropwise at 0 °C to a solution of ethylenediamine (4.0 mL, 59.9 mmol, 5.3 eq) in 20 mL anhydrous DCM under nitrogen. The reaction was allowed to warm up to room temperature while stirring over night before it was quenched with excess water (10 mL). The phases were separated and the water phase extracted twice with $CHCl_3$. The combined organic layers were washed three times with saturated NaCl, three times with saturated $K_2CO_3$ and dried with $MgSO_4$. The solvent was removed under reduced pressure and a white solid was obtained. The crude product was purified by column chromatography ($CHCl_3$/MeOH 9:1, with trace TEA) which was monitored with TLC (stain: 20 vol-% $H_2SO_4$). The solvent was removed under reduced pressure and a white solid was obtained (3.84 g, 8.13 mmol, 73 % yield). R$_f$: 0.51 ($CHCl_3$/MeOH 4:1); $^1$H NMR (500 MHz, $CDCl_3$): δ = 5.36 (d, *J* = 5.2 Hz, 1H, H-6), 5.05 (t, *J* = 5.7 Hz, 1H, NH), 4.57 – 4.37 (m, 1H, H-3), 3.25-3.19 (m, 2H, H-1´), 2.89 – 2.73 (m, 2H, H-2´), 2.38 – 2.22 (m, 2H, H-24), 2.02 – 1.78 (m, 5H, H-2, H-7, H-8), 1.60 – 1.03 (m, 21H, H-1, H-4, H-9, H-11, H-12, H-14, H-15, H-16, H-17, H-20, H-22, H-23, H-25), 1.00 (s, 3H, H-19), 0.90 (d, *J* = 6.5 Hz, 3H, H-21), 0.86 (dd, *J* = 6.6, 2.3 Hz, 6H, H-26, H-27), 0.67 (s, 3H, H-18) ppm.; $^{13}$C NMR (126 MHz, $CDCl_3$): δ = 156.6(NCOO), 140.0 (C-5), 122.6 (C-6), 74.4 (C-3), 56.8 (C-14), 56.3 (C-17), 50.1 (C-9), 43.7 (C-1´), 42.4 (C-2`), 41.9 (C-13), 39.8 (C-12), 39.6 (C-4), 38.7 (C-24), 37.1 (C-1), 36.7 (C-10), 36.3 (C-22), 35.9 (C-20), 32.0 (C-8), 32.0 (C-7), 28.4 (C-25), 28.3 (C-20), 28.1 (C-16), 24.4 (C-15), 24.0 (C-23), 23.0 (C-27), 22.7 (C-26), 21.2 (C-11), 19.5 (C-19), 18.8 (C-21), 12.0 (C-18) ppm; HRMS: calc. for $C_{30}H_{52}N_2O_2$ [m + H]$^+$ : 473.4107, found [m + H]$^+$: 473.4100

**Post-modification of reactive poly(pentafluorphenyl methacrylate) particles** Freeze-dried PPFPMA particles (400 mg, 1.59 mmol w.r.t monomer units of PPFPMA particles, 1.0 eq) were dispersed in 80 mL DMF by short treatment in a sonication bath. The particles were swollen overnight in DMF before different molar ratios of amine functionalized moieties (3.0 eq w.r.t. monomer units, Table S- 3) and TEA (660 µL, 4.77 mmol, 3.0 eq w.r.t. monomer units) were added and heated to 50 °C for 24 hours. Afterwards the nanogels were purified by

extensive dialysis first against DMF (1 week) and subsequently against DI water (1 week) and ultrapure water (1 week). The nanogels were then freeze-dried and obtained as white powder.

The nanogels can be stored and redispersed in DI water or phosphate-buffered saline (PBS) by vortex and short sonication treatment. The success of the post-modification reaction was monitored by ATR-FTIR spectroscopy on freeze-dried nanogels.

The size of the amphiphilic nanogels after post-modification was determined by dynamic light scattering after redispersion of the freeze-dried samples in DI water.

**Table S- 3** post-reaction of particles.
Parameters for modification PPFPMA precursor
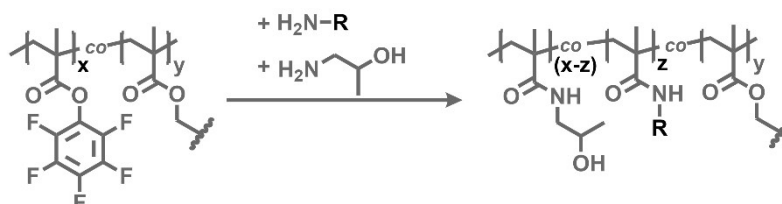


| Sample name | HPA | | | Hydrophobic group R | | | |
|---|---|---|---|---|---|---|---|
| | eq | n [mmol] | m [mg] | Type of hydrophobic group R | eq | n [mmol] | m [mg] |
| PHPMA | 3 | 4.76 | 358 | - | - | - | - |
| BENZA-20 | 2.4 | 3.81 | 286 | BENZA | 0.6 | 0.95 | 102 |
| HEXA-20 | 2.4 | 3.81 | 286 | HEXA | 0.6 | 0.95 | 96 |
| BDODA-20 | 2.4 | 3.81 | 286 | BDODA | 0.6 | 0.95 | 176 |
| DODA-20 | 2.4 | 3.81 | 286 | DODA | 0.6 | 0.95 | 176 |
| CHOLA-10 | 2.7 | 4.28 | 322 | CHOLA | 0.3 | 0.48 | 225 |
| CHOLA-20 | 2.4 | 3.81 | 286 | CHOLA | 0.6 | 0.95 | 450 |
| CHOLA-30 | 2.1 | 3.33 | 250 | CHOLA | 0.9 | 1.43 | 675 |
| CHOLA-40 | 1.8 | 2.86 | 215 | CHOLA | 1.2 | 1.90 | 900 |
| CHOLA-50 | 1.5 | 2.38 | 179 | CHOLA | 1.5 | 2.38 | 1124 |

**Synthesis of poly(pentafluorophenyl methacrylate) (PPFPMA)**[1] In a predried schlenk flask PFPMA (1.00 g, 3.96 mmol, 1.0 eq) and AIBN (6.5 mg, 0.04 mmol, 0.01 eq) were dissolved in 2 mL anhydrous toluene under nitrogen. The reaction mixture was degassed by bubbling nitrogen through the solution for 30 min before heating to 75 °C for 20 hours under nitrogen. The product was purified by precipitating twice in cold methanol. The product was obtained as a white solid in a yield of 70 % (0.71 g).^{1}H NMR (400 MHz, CDCl$_3$): δ = 2.41 (br s, 2H, -CH$_2$), 1.48 – 1.20 (m, 3H, -CH$_3$)ppm; ^{19}F NMR (376 MHz, CDCl$_3$): δ = -150.34 (d, $J$ = 60.9 Hz, 1F, F$_{ortho}$), -151.39 (s, 1F, F$_{ortho}$), -156.88 (s, 1F, F$_{para}$), -162.03 (s, 2F, F$_{meta}$) ppm; GPC M$_n$ = 19700 Da, M$_w$ = 34700 Da, PDI = 1.76; IR (ATR-FTIR): ũ = 2996 (w), 2460 (w), 1778 (m, C=O), 1654 (w), 1515 (s), 1470 (m), 1397 (w), 1362 (w), 1316 (w), 1246 (w), 1048 (s), 990 (s), 857 (w), 734 (w), 715 (w), 661 (w) cm$^{-1}$.

**Post-polymerization modification of reactive poly(pentafluorphenyl methacrylate)**[5] PPFPMA (50 mg, 0.20 mmol w.r.t. monomer units, 1.0 eq) was dissolved in 10 mL DMF by short treatment in a sonication bath. For the simultaneous addition different molar ratios of amine functionalized moieties (3.0 eq w.r.t. monomer units, see Table S- 4) and TEA (82 µL, 0.6 mmol 3.0 eq w.r.t. monomer units) were added and heated to 50 °C for 24 hours.

For the sequential experiments, CHOLA (0.1 - 0.5 eq w.r.t. monomer units, Table S- 4) and TEA (82 µL, 0.6 mmol 3.0 eq w.r.t. monomer units) were added and heated to 50 °C. After 24 h an excess of HPA was added and the reaction was conducted for another 24 hours.

Afterwards the polymers were purified by extensive dialysis first against DMF (1 week) and subsequently against DI water (2 weeks). The polymers were then freeze dried and obtained as white powder. The success of the post-modification reaction was monitored by ATR-FTIR spectroscopy on freeze dried polymers. The incorporation efficiencies of the functional moieties were determined by ^{1}H NMR.

**Table S- 4** Parameters for post-modification reaction of PPFPMA polymers.
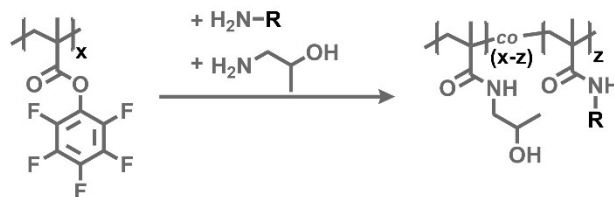


| Experimental setup | Sample name | eq | n [mmol] | m [mg] | Type of hydrophobic group R | eq | n [mmol] | m [mg] |
|---|---|---|---|---|---|---|---|---|
| simultaneous | PHPMA | 3 | 0.60 | 45 | - | - | - | - |
| | CHOLA-10 | 2.7 | 0.54 | 41 | CHOLA | 0.3 | 0.06 | 28 |
| | CHOLA-20 | 2.4 | 0.48 | 36 | CHOLA | 0.6 | 0.12 | 57 |
| | CHOLA-30 | 2.1 | 0.42 | 32 | CHOLA | 0.9 | 0.18 | 85 |
| | CHOLA-40 | 1.8 | 0.36 | 27 | CHOLA | 1.2 | 0.24 | 113 |
| | CHOLA-50 | 1.5 | 0.30 | 23 | CHOLA | 1.5 | 0.30 | 142 |
| sequential | PHPMA | 3 | 0.60 | 45 | - | - | - | - |
| | CHOLA-10 | 2.9 | 0.58 | 44 | CHOLA | 0.1 | 0.02 | 9 |
| | CHOLA-20 | 2.8 | 0.56 | 42 | CHOLA | 0.2 | 0.04 | 19 |
| | CHOLA-30 | 2.7 | 0.54 | 41 | CHOLA | 0.3 | 0.06 | 28 |
| | CHOLA-40 | 2.6 | 0.52 | 39 | CHOLA | 0.4 | 0.08 | 38 |
| | CHOLA-50 | 2.5 | 0.50 | 38 | CHOLA | 0.5 | 0.10 | 47 |

**References:**

1.    M. Eberhardt, R. Mruk, R. Zentel and P. Théato, *European Polymer Journal*, 2005, **41**, 1569-1575.
2.    J.-C. Blazejewski, J. W. Hofstraat, C. Lequesne, C. Wakselman and U. E. Wiersum, *Journal of Fluorine Chemistry*, 1998, **91**, 175-177.
3.    Y. Nie, M. Günther, Z. Gu and E. Wagner, *Biomaterials*, 2011, **32**, 858-869.
4.    M. D. Kearns, A.-M. Donkor and M. Savva, *Molecular Pharmaceutics*, 2008, **5**, 128-139.
5.    M. I. Gibson, E. Fröhlich and H.-A. Klok, *Journal of Polymer Science Part A: Polymer Chemistry*, 2009, **47**, 4332-4345.